

FIRST HIGH-GRADIENT RESULTS OF UED/UEM SRF GUN AT CRYOGENIC TEMPERATURES*

R. Kostin[†], C. Jing, Euclid Beamlabs LLC, Bolingbrook, IL, USA
S. Posen, T. Khabiboulline, D. Bice, Fermilab, Batavia, IL, USA

Abstract

Benefiting from the rapid progress on RF photogun technologies in the past two decades, the development of MeV range Ultrafast Electron Diffraction/Microscopy (UED and UEM) has been identified as an enabling instrumentation. UEM or UED use low power electron beams with modest energies of a few MeV to study ultrafast phenomena in a variety of novel and exotic materials. SRF photoguns become a promising candidate to produce highly stable electrons for UEM/UED applications because of the ultrahigh shot-to-shot stability compared to room temperature RF photoguns. SRF technology was prohibitively expensive for industrial use until two recent advancements: Nb₃Sn and conduction cooling. The use of Nb₃Sn allows to operate SRF cavities at higher temperatures (4 K) with low power dissipation which is within the reach of commercially available closed-cycle cryocoolers. Euclid is developing a continuous wave (CW), 1.5-cell, MeV-scale SRF conduction cooled photogun operating at 1.3 GHz. In this paper, we present first high gradient results of the gun conducted in liquid helium.

INTRODUCTION

The use of SRF photogun brings certain benefits compared to normal conducting guns such as: unprecedented repetition rates (CW), reduced almost to zero RF losses, higher RF stability. As long as beam current is very low for UED/UEM applications, MW-level RF power source is not required and can be as low as several Watts. However, SRF was not user-friendly because it requires sophisticated cryomodules, experienced personnel and expensive cryogenics until recent proof of principle of conduction cooling at Fermilab [1], in which Euclid participated and Jlab [2].

Euclid is developing a CW, 1.5-cell L-band conduction-cooled SRF photogun operating at 1.3 GHz for UED/UEM applications [3,4]. The design of the gun was initially based on an existing cavity with an "on-axis" coaxial coupler developed by Euclid [5], however it was later changed to a standard Tesla end-cell with side couplers [6] to lower manufacturing costs. No beam quality degradation has been found in simulations. The half-cell geometry was optimized using CST, which was bench marked by ASTRA code. The beam parameters were optimized and are suitable for UED/UEM [7]. Beam energy out of the gun is 1.65 MeV which requires field on the cathode (on axis) of 20 MV/m. This field corresponds to accelerating gradient of 10 MV/m and can be found in Fig. 1.

* Work supported by US DOE SBIR grant DE-SC0018621.

[†] r.kostin@euclidtechlabs.com

Eigenfrequency=1.3 GHz Volume: emw.normE*Escl (MV/m)

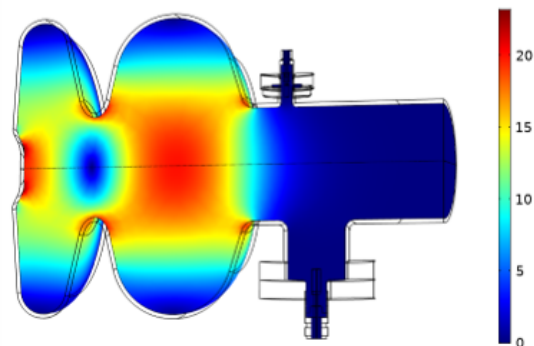


Figure 1: E-field distribution in the gun at $E_{acc}=10$ MV/m.

The RF dissipated power is below 1 W at quality factor of $Q_0=1.1 \times 10^{10}$ and accelerating gradient of 10 MV/m. This field level and quality factor is achievable nowadays even for 9-cell Tesla cavity [8]. The gun will be cooled using welded Nb equator rings - Fermilab's conduction cooling approach developed in collaboration with Euclid [9]. The "dry" cryomodule has been developed and is ready to host the cavity (see details in Ref. [4]) once the gun performance covered with Nb₃Sn is demonstrated in liquid helium at 4 K.

THE GUN TUNING

Tuning fixtures were designed to tune the gun field balance and frequency and can be found in Fig. 2.

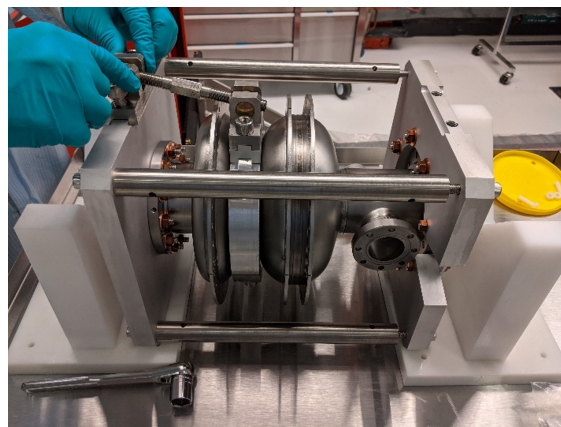


Figure 2: 1.5 cell Nb SRF gun with cooling rings welded.

The fixtures consist of: turnbuckle-style connecting rods, side aluminium plates, split ring installed on the gun iris, longitudinal titanium rods. The fixtures without the split ring and turnbuckles is used for cavity support under vacuum

Content from this work may be used under the terms of the CC BY 4.0 licence (© 2022). Any distribution of this work must maintain attribution to the author(s), title of the work, publisher, and DOI

including during cryogenic tests. That is why it needs to match thermal expansion of the gun (titanium CTE is very close to niobium) and made from non-magnetic material. The half cell need additional reinforcement as the gun yield stress is expected to be as low as 20 MPa after Nb₃Sn deposition as it happens at very high temperatures. The principle of tuning is based on longitudinal push-pull of the individual cells actuated by the turnbuckle rods. The plate on the right can be left free or fixed depending on tuning configuration.

The gun frequency should be tuned to 1300.20 MHz to obtain the required frequency for the cryogenic test. Table 1 below, demonstrates the frequency change due to BCP, vacuum evacuation and temperature change.

Table 1: Gun Frequency Change, F_s - simulated, F_m - measured, $\Delta F = F_m - F_s$

Case	F_s , MHz	F_m , MHz	ΔF , MHz
300 K, air	1300.20	1300.50	0.30
300 K, air, BCP	1297.80	1299.48	1.68
300 K, vac, BCP	1298.20	1301.58	3.38
002 K, vac, BCP	1300.00	1303.48	3.48

The frequency change was simulated first and compared to measured values. Expected frequency change due to 200 μ m BCP is -2.4 MHz, air evacuation is +0.40 MHz, cool down from 300 K to 2 K is +1.8 MHz taking into account Nb CTE=0.143%.

Initial gun frequency as received was 1301.27 MHz with field in the full cell of 80% of the required level (by design, the field on axis in the half cell is -2.6% lower than in the full cell) and is presented in Fig. 3.

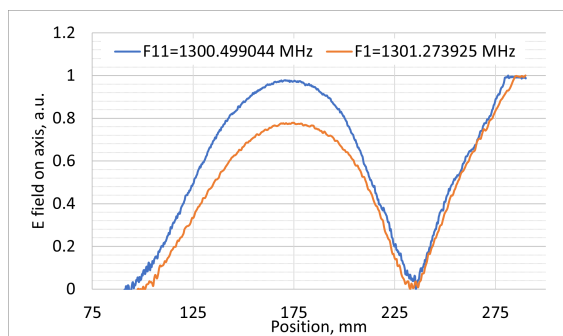


Figure 3: 1.5 cell Nb SRF gun field balance and frequency tuning results.

It took 11 consequent push-pulls of different cells to bring the field balance and frequency to the required values. At the end the frequency was tuned to 1300.50 MHz, a little bit higher than needed (see the first row in Table 1).

After the gun was tuned, it obtained close to 200 μ m BCP and was high power tested. The frequencies at each step were recorded and can be found in Table 1 (see the third column). It was found that BCP caused more than two times lower frequency shift of -1.02 MHz. The gun frequency under vacuum was additionally reduced by -1.7 MHz. It

was found that the support fixtures stressed the cavity which resulted in this frequency shift. This issue was recognized and solved in consequent experiments. The gun frequency change due to the cool down was very close to the expected value and equaled to +1.9 MHz.

THE GUN INITIAL PROCESSING

The cavity thickness was measured after manufacturing and found to be around 2.9 mm thick. The gun was processed at Argonne-Fermilab joint facility and received the following treatment:

- 150 μ m rotational BCP
- 800 °C bake for 3 hours
- 40 μ m BCP

The inner surface of the cavity before and after the processing can be found in Fig. 4.

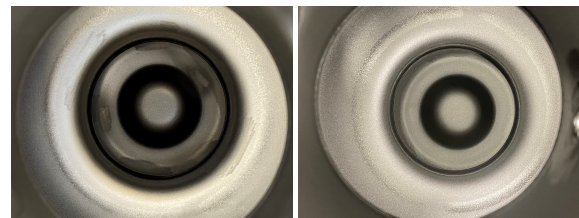


Figure 4: 1.5 cell SRF gun inner surface before and after BCP.

As one can see, initial surface mechanical grinding of imperfections are completely gone. The gun removed layer was measured in several places which can be found in Fig. 5. The results are summarized in Table 2 below. The etched layer is fairly uniform and is around 200 μ m thick which is greater than the minimum recommended thickness of 120 μ m.

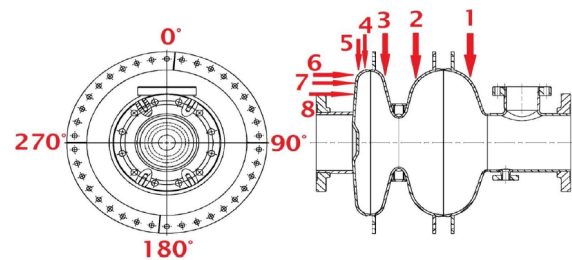


Figure 5: The gun thickness measured points.

The gun was manually cleaned by HPR with a nozzle which had sprays 22.5° degree from the gun axis. This set up usually is good enough for cavities when cleaned from both sides, however as long as our gun geometry has opening only from one side it appeared to be not sufficient enough as was found later.

PURE NB GUN TEST AT 2 K

The cavity was tested in a vertical cryostat at Fermilab. One can find the "Q versus E" curve in Fig. 6. Accelerating gradient of 10 MV/m was achieved during this very first test

Table 2: Removal Layer Thickness in μm

Point	0	90	180	270
1	229	193	211	192
2	276	294	254	261
3	223	195	219	208
4	212	222	238	208
5	228	231	246	193
6	204	170	200	197
7	185	187	206	160
8	164	168	202	180

which is the target operating gradient at 4 K, however the quality factor at low fields was low quite low, equaled to $Q_0=2.6 \times 10^9$ degrading after 7 MV/m because of increasing field emission. Radiation was also recorded and presented on Fig. 6 as well. Multipactor was not present up to the operating gradient. Several quenches happened due to field emission but the test was power limited as most of the power reflected from the gun (200 W): external Q-factor was tuned for $Q_0=1 \times 10^{10}$ which was significantly lower. The gun was tested at 1.4 K as well and it was discovered that lower temperature did not improve quality factor meaning that the losses were dominated by high residual resistance.

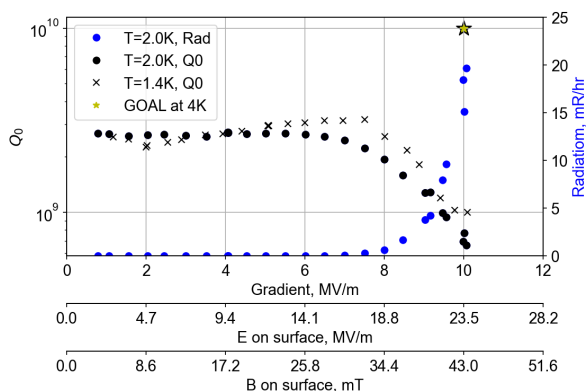


Figure 6: Results of test 1 in liquid helium bath.

One can conclude from the first test that the cavity surface was probably required more thorough cleaning. In preparation for the next 2 K test, the gun received $10 \mu\text{m}$ BCP and most importantly automatic HPR with a new nozzle which provided a better surface treatment. The nozzle had two sprays at 90° and 60° degree from the cavity axis which provided more surface coverage. The results of the second test are presented in Fig. 7.

Accelerating gradient of 22 MV/m was achieved during the second test and the quality factor was greatly improved up to $Q_0=1.2 \times 10^{10}$ with no degradation at higher gradients. The test reached twice the operating gradient and was stopped as proved to be sufficiently high. No multipactor or field emission were observed. The gun was tested at 1.5 K as well and a significant Q-factor improvement was observed.

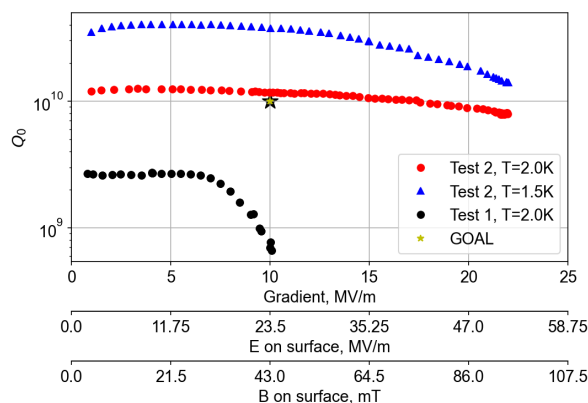


Figure 7: Results of test 1 and 2 in liquid helium bath.

One can conclude that the changes in surface processing significantly improved the performance.

FUTURE PLANS

The gun will be covered with Nb_3Sn and tested in Fermilab's vertical stand with the goal to demonstrate high $Q_0=1 \times 10^{10}$ at $E_{\text{acc}}=10$ MV/m and 4 K. The next stage will include the gun test at Euclid using conduction cooled cryomodule. The final goal of this project is the development of UED/UEM user facility in Brookhaven national laboratory in ATF-II bunker. The initial agreement is already obtained. Once the gun performance is demonstrated the whole system will be delivered to BNL where a beam line will be assembled for beam generation and characterization.

CONCLUSION

Several key milestones towards UED/UEM facility based on conduction cooled SRF photogun have been accomplished:

- The pure Nb gun demonstrated high $Q_0=1 \times 10^{10}$ at 2 K.
- Reached $E_{\text{acc}}=22$ MV/m which is 2 times higher than the required operating gradient.
- Exceptional performance of the bare gun was demonstrated.
- The gun is ready for Nb_3Sn deposition.
- Successful cleaning procedure has been established.

ACKNOWLEDGMENTS

We would like to thank the Department of Energy Small Business Innovation Research office for their support provided to conduct the research: grant #DE-SC0018621. We would also like to thank the technical staff at Argonne National Laboratory and Fnal's APST Division and for the cavity preparation and Dr. A. Netepenko for the RF test of the cavity.

REFERENCES

- [1] R. C. Dhuley, S. Posen, O. Prokofiev, M. I. Geelhoed, and J. C. T. Thangaraj, "First demonstration of a cryocooler conduction-

- cooled superconducting radiofrequency cavity operating at practical cw accelerating gradients”, *Supercond. Sci. Technol.*, vol. 33, no. 6, p.06LT01, Apr. 2020.
doi:10.1088/1361-6668/ab82f0
- [2] G. Ciovati *et al.*, “Multi-metallic conduction cooled superconducting radio-frequency cavity with high thermal stability”, *Supercond. Sci. Technol.*, vol. 33, no. 7, p. 07LT01, May 2020.
doi:10.1088/1361-6668/ab8d98
- [3] R.Kostin *et al.*, “Conduction cooled SRF photogun for UEM/UED applications”, presented at the 23rd ATF user meeting, Virtual Event, Dec. 2020, proposal UED308081.
- [4] R. A. Kostin, P. V. Avrakhov, C. Jing, A. Liu, and Y. Zhao, “Status of Conduction Cooled SRF Photogun for UEM/UED”, in *Proc. IPAC’21*, Campinas, Brazil, May 2021, pp. 1773–1776. doi:10.18429/JACoW-IPAC2021-TUPAB167
- [5] Y. Xie *et al.*, “Demonstration of Coaxial Coupling Scheme at 26 MV/m for 1.3 GHz Tesla-Type SRF Cavities”, in *Proc. SRF’15*, Whistler, Canada, Sep. 2015, paper THPB105, pp. 1397–1399.
- [6] B. Aune *et al.*, “The Superconducting TESLA Cavities”, *Phys. Rev. Spec. Top. Accel Beams*, vol. 3, no. 9, p. 092001, Sep. 2000.
doi:10.1103/PhysRevSTAB.3.092001
- [7] A. Liu, P. V. Avrakhov, C. Jing, and R. A. Kostin, “Optimization of an SRF Gun Design for UEM Applications”, in *Proc. NAPAC’19*, Lansing, MI, USA, Sep. 2019, pp. 305–308.
doi:10.18429/JACoW-NAPAC2019-TUYBA4
- [8] S.Posen *et al.*, “Advances in Nb₃Sn superconducting radiofrequency cavities towards first practical accelerator applications”, *Supercond. Sci. Technol.*, vol. 34, no. 2, p. 025007, Jan. 2021.
doi:10.1088/1361-6668/abc7f7
- [9] R. Dhuley *et al.*, “Thermal Link Design for Conduction Cooling of SRF Cavities Using Cryocoolers”, *IEEE Trans. Appl. Supercond.*, vol. 29, no. 5, pp. 1–5, Aug. 2019.
doi:10.1109/TASC.2019.2901252